An Improved Minimum-cost Charging Schedule for Large-Scale Penetration of Electric Vehicles

Wenping Zhang, Caleb Dreise, Riming Shao, and *Liuchen Chang*
Emera & NB Power Research Centre for Smart Grid Technologies, Dept. of Electrical and Computer Engineering, University of New Brunswick, Fredericton, NB, Canada, E3B 5A3
wzhang18@unb.ca

***Abstract*—Plug-in electric vehicles (EVs) have been considered as one of the important facilitators for reducing greenhouse gas emissions. With the growth of EV penetrations, uncoordinated charging scheduling could aggravate the grid load and thus smart charging management is becoming critical. In this paper, an EV charging cost model is first built, which takes into account the electricity rates, EV mobility, and EV battery and charger specifications. Then, the evaluation of the conventional charging schedule associated with minimizing users' cost is presented and two primary issues are illustrated including power surges and aggravated dynamic response for the grid. Furthermore, an improved minimum-cost strategy is proposed to mitigate these two issues and the corresponding algorithm is illustrated. Finally, the simulation results are provided to validate the proposed strategy.**

Keywords— Plug-in electric vehicles, smart charging, minimum cost, power surge

I. Introduction

Climate change and global warming due to greenhouse gas emissions have been posing a negative impact on human society and thus greenhouse gas reduction has become one of world's common goals. Plug-in electric vehicles (EVs) have been considered as one of the important scenarios for reducing greenhouse gas emissions[1]. Additionally, EVs can play an important role in future smart grid systems[2]-[3], such as peak shaving and valley filling, spinning reserve, frequency and voltage regulation service, energy storage for renewable energy, and current harmonic filtering. Also, numerous papers have investigated EV management issues when interfacing with the grid, including *State of charge* (SOC) management, owning revenue through energy arbitrage, battery cycle management and lifespan extension, and smart charging[4]. Among them, smart charging management is becoming critical, since uncoordinated charging scheduling could affect the grid's operating performance and increase the operating costs, especially with the growth of EV penetrations.

Numerous charging scheduling strategies have been proposed, which basically fall into three categories. The first category is from the grid's perspective, and the optimization objectives include minimizing grid operating cost, total power loss, errors between actual load and the target, and load variance, and maximizing profits while minimizing energy trading risks[5]-[6]. The second category is from users' perspective, and the optimization objectives involve minimizing charging cost, minimizing both CO_2 emission and charging cost, maximizing EVs' average SOC, maximizing users' convenience[7]-[8], etc. In addition, a few papers jointly optimize the benefits of both grid-side and EV-side[9]. In order to achieve these optimization objectives, various optimization algorithms have been introduced[1]-[9], such as convex optimization, linear programming, quadratic programming, game theoretic approach, swarm particle optimization, heuristic methods, and mixed integer stochastic optimization. Also, different constraints have been applied for the optimization. On the grid-side, the constraints such as power balance, voltage or line thermal limits, and upstream supplier limits, have been applied. Also, for the EV-side, the constraints, such as battery power rate of change limit, battery SOC, and EV availability, are applied. Furthermore, the EV mobility pattern is investigated in a few papers [10], such as EV arrival & departure time, trip history and unplanned departure, which is more realistic, but more complex. Among the proposed scheduling, the minimum users' cost scheduling is commonly applied. However, few papers have analyzed the impacts of EV charging behavior on the grid, especially in cases of large-scale penetrations. Therefore, this paper investigates the negative impacts of the convention minimum-cost scheduling on the grid and proposes an improved scenario to mitigate the negative impacts.

The main features of this paper are,

a) A mathematical charging cost model is built, and the related factors shown in Fig.1 are taken into account.

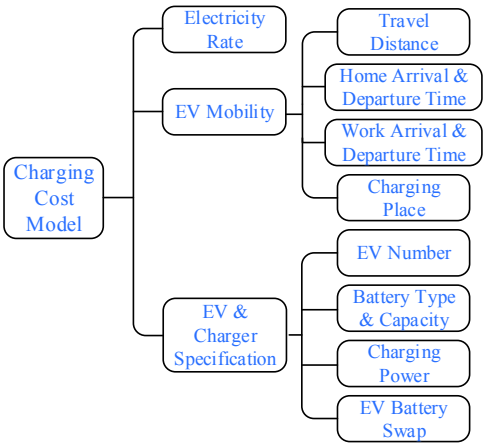

Fig. 1 Factors for EV charging cost model

b) The proposed minimum-cost scheduling strategy preferentially charges EVs in lighter load zones under an equal price guarantee. As a result, the power surge caused by the

conventional scheduling strategies can be suppressed significantly.

c) The proposed strategy can reduce the grid power change rate via limiting the power ramping rate of the EV. This can improve the dynamic performance of the grid and reduce the operating costs of the grid, which are caused by the conventional scheduling strategies.

II. EV Charging Cost Model

A. Electricity Rate

The TOU electricity rates during summer weekdays, winter weekdays and weekends & holidays in Ontario, Canada are presented in Fig. 2. The different electricity rates make it possible for EV users to own the revenue with a smart scheduling.

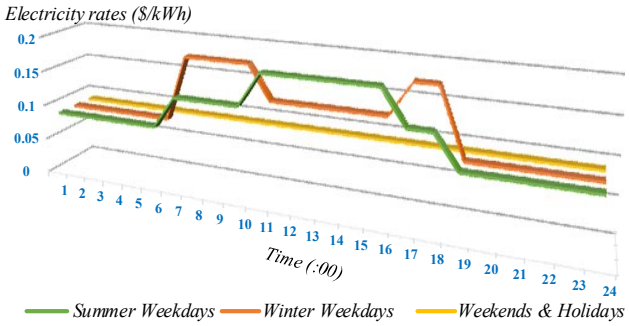

Fig. 2 TOU electricity rates in Ontario, Canada

B. EV Mobility

A typical EV daily mobility pattern is presented in Fig. 3. The factors, including *daily travel distance, home arrival & departure time*, and *work arrival & departure time,* are analyzed in the following.

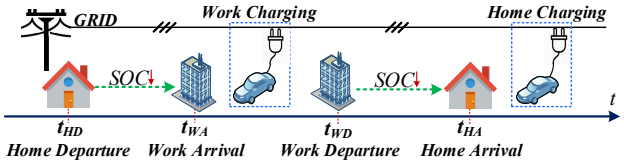

Fig. 3 EV daily mobility pattern

- *Daily Travel Distance*

The daily travelling distance L is typically modelled as a log-normal distribution[11],

$$f_D(L) = \frac{1}{\sqrt{2\pi}\sigma_D L} e^{\left[-\frac{(\ln L-\mu_D)^2}{2\sigma_D^2}\right]} \quad (1)$$

where μ_D= 3.4 and σ_D= 0.5.

Assuming that the EV energy consumption rate is 30kWh per 100 miles, EV daily remaining *SOC* S_R before the charging can be described as,

$$S_R = 1 - \frac{L}{100} \times \frac{30}{E_{full}} \quad (2)$$

where E_{full} is the EV battery energy capacity.

If E_{full} is 30kWh, with (1) and (2), the probabilities of the daily distance (f_D) and remaining SOC (f_{SOC}) are presented in Fig. 4.

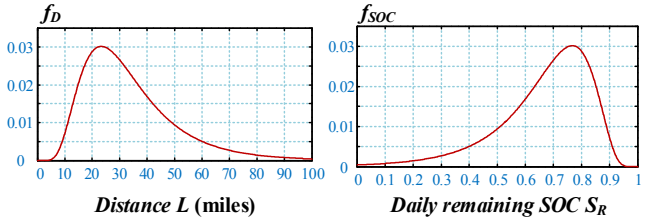

Fig. 4 Probabilities of the daily distance and remaining SOC

- *Home Arrival & Departure Time*

The probabilities of the EV home arrival time (f_{HA}) and home departure time (f_{HD}) are modelled as normal distributions[12], which are shown in (3)-(4).

$$f_{HA}(t_{HA}) = \begin{cases} \frac{1}{\sqrt{2\pi}\sigma_{HA}} e^{\left[-\frac{(t_{HA}-\mu_{HA})^2}{2\sigma_{HA}^2}\right]}, \mu_{HA} - 12 < t_{HA} \le 24 \\ \frac{1}{\sqrt{2\pi}\sigma_{HA}} e^{\left[-\frac{(t_{HA}+24-\mu_{HA})^2}{2\sigma_{HA}^2}\right]}, 0 < t_{HA} \le \mu_{HA} - 12 \end{cases} \quad (3)$$

$$f_{HD}(t_{HD}) = \begin{cases} \frac{1}{\sqrt{2\pi}\sigma_{HD}} e^{\left[-\frac{(t_{HD}-\mu_{HD})^2}{2\sigma_{HD}^2}\right]}, 0 < t_{HD} \le 12 + \mu_{\mathrm{HD}} \\ \frac{1}{\sqrt{2\pi}\sigma_{HD}} e^{\left[-\frac{(t_{HD}-24-\mu_{HD})^2}{2\sigma_{HD}^2}\right]}, 12 + \mu_{\mathrm{HD}} < t_{HD} \le 24 \end{cases} \quad (4)$$

where μ_{HA}= 17.6, μ_{HD} = 8.92, σ_{HA} = 3.4, and σ_{HD}= 3.24.

With (3) and (4), Fig. 5 presents the probabilities of the home arrival time and departure time.

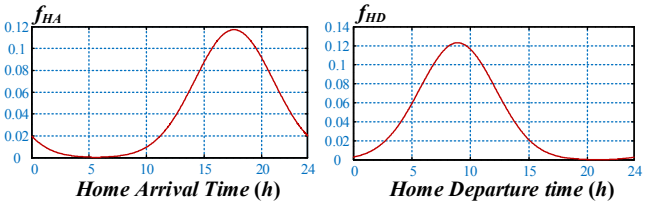

Fig. 5 Probabilities of the home arrival and departure time

- *Work Arrival & Departure Time*

Suppose that the average travelling speed is 20 miles per hour (*mph*). With the daily travelling distance in (1), the average time spent on the road Δt can be obtained. With Δt, the work arrival time (t_{WA}) and work departure time (t_{WD}) can be expressed as,

$$\begin{cases} t_{\mathrm{WA}} = t_{\mathrm{HD}} + \Delta t/2 \\ t_{\mathrm{WD}} = t_{\mathrm{HA}} - \Delta t/2 \end{cases} \quad (5)$$

Then, based on (3) ~ (5), the probabilities of the work arrival time (f_{WA}) and work departure time (f_{WD}) can be obtained, as shown in Fig. 6.

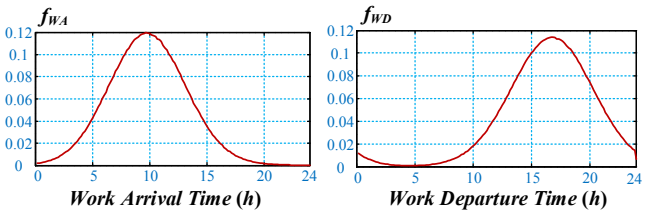

Fig. 6 Probabilities of the work arrival time and departure time

C. Electric Vehicle & Charger Specifications

The Nissan Leaf, with a battery capacity of 30 *kWh*, is used as a standard model in this paper because it has the largest market share in the world. For household cars, *level II* chargers are normally applied and the corresponding charging models are presented in Fig. 7.

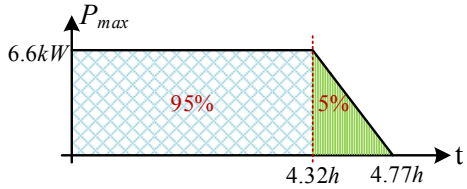

Fig. 7 Charging models for level II

The EV charging power P_{EV} must be lower than the maximum power (P_{max}) as present in (6).

$$P_{EV} \leq P_{max} \tag{6}$$

In this paper, the number of EVs is based on different penetration, which is assumed to be 10%, 20%, etc., of the current number of total cars in Ontario (approximately 6,727,791) for the case study.

III. Evaluation of Conventional Minimum-Cost Charging Schedule

Based on the analysis in Section II, the system specifications are presented in Table. I. Note that the home charging is taken as an example for the analysis. Also, each EV's daily travelling distance L, and the home arrival and departure time t_{HA} and t_{HD} are randomly assigned based on the distribution in (2)-(4).

Table. I System specifications

Items	Specifications
Grid Load Profile	*Data from Ontario, Canada*
TOU Price	*Ontario, Canada (Fig. 2)*
Electric Vehicle	*Nissan leaf, 30kWh*
EV Chargers	*Level II (6.6kW)*
Charging Places	*Home*
EV Mobility Pattern	*Using the built model (see Part II.B)*
EV Penetration	10%, 20%, etc., of 6,727,791

Using the mathematical model in Section II and the specification in *Table. I*, two charging scheduling strategies are compared. 1) The *uncoordinated scheduling* charges the battery as soon as the EV is plugged into the grid. 2) The *conventional minimum-cost scheduling* minimizes the users' charging cost, where the battery is charged in the low-price zone and discharged in the high-price zone. The EV user costs for different scheduling strategies in the case of home charging are shown Fig. 8.

It is known that, with the minimum-cost scheduling, the charging power is clustered into the low-price time zone to reduce the cost. Therefore, in Fig. 8, the corresponding cost is reduced with the minimum-cost scheduling. Additionally, the bi-directional charger can discharge the power in the high-price zone, which further reduced the costs for the users. Specifically, the charging cost for bi-directional chargers is decreased to \$0.3/day per EV.

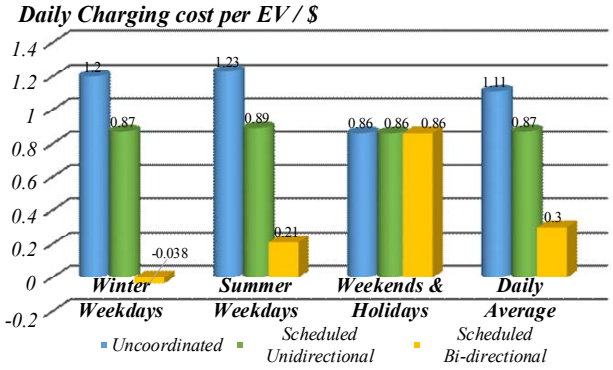

Fig. 8 Comparison of the daily cost for different strategies (Home charging)

However, for the minimum-cost charging, most users intend to charge their EV as soon as the price drops into the low-price zone. Therefore, a great power surge will occur at the time when the low-price zone starts. Fig. 9 presents the results of the grid load with different scheduling and under different EV penetrations. There is a big power surge at 19:00 when the time starts to enter low-price zone for the minimum-cost scheduling. It is also observed that this power surge is becoming worse with the increase of the EV penetrations.

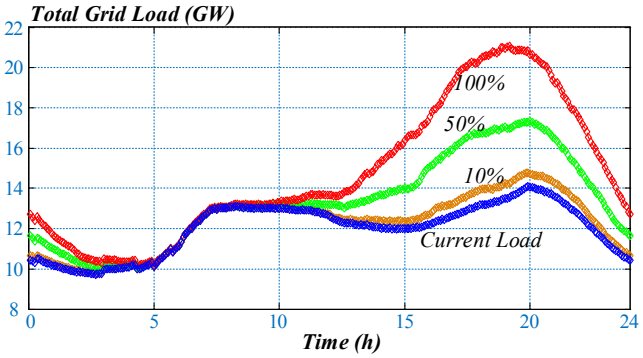

(a) Uncoordinated scheduling

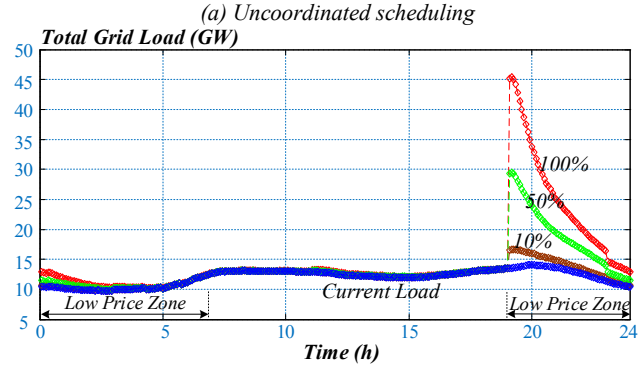

(b) Min-cost scheduling (Unidirectional)

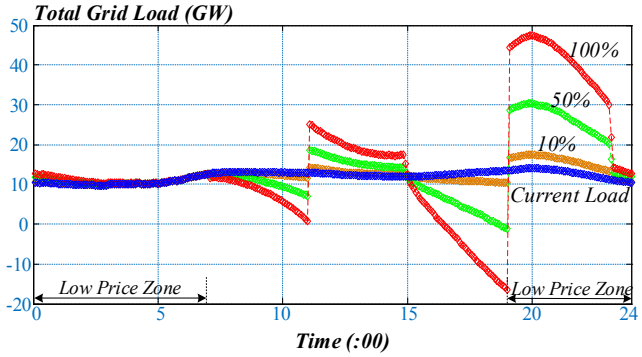

(c) Min-cost scheduling (Bi-directional)

Fig. 9 The grid load with the increase of EV penetration (Home charging)

There are two drawbacks for this power surge:

1) The load of the grid is aggravated, and thus the grid's capacity needs to be expanded to deal with this issue. The maximum power load with the increase of EV penetration is presented in Fig. 10. It can be seen that the grid capability has to approximately expand to 3.5 times of the original size for the 100% EV penetration.

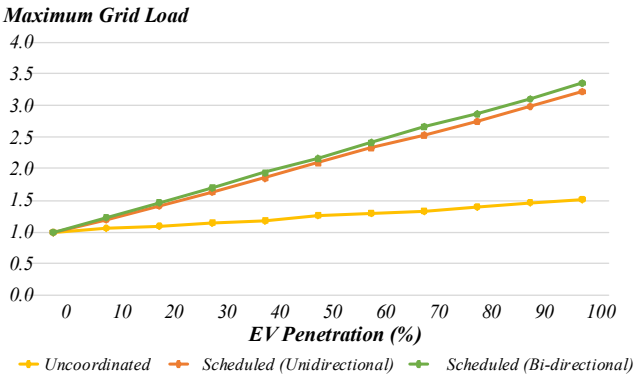

Fig. 10 Maximum power load with an increase of EV penetration (Note: the maximum power is uniformed and the base is the maximum power when the penetration is 0%.)

2) As shown in Fig. 9, the ramp rate of the load is increased greatly as well. In order to cope with this fast response, the grid has to simultaneously ramp up or ramp down the output power. As a result, the system operating cost will be enhanced to deal with the fast dynamic response. Also, the system reliability is reduced significantly.

IV. Improved Minimum-Cost Charging Schedule

From section III, there are two problems regarding the conventional min-cost scheduling, including the aggravated loads and fast dynamic requirements. Therefore, an improved strategy is proposed to cope with these two issues.

A. Mathematical Functions

There are two optimization objectives for the improved strategy. The first objective is still to minimize the total charging cost (C_{EV}). Additionally, a minor objective is added to lower the maximum grid load (P_{G_max}). Taking home charging as an example, the expressions are presented in (7)-(8).

$$min\ [C_{EV} = \int_{t_{HA}}^{t_{HD}} M(t) P_{EV\_Conv}(t) dt] \tag{7}$$

$$min\ [P_{G\_max} = max\ (P_G + P_{EV\_Conv})] \tag{8}$$

where M is the electricity TOU price, P_{EV} is the EV charging power (see (11)) and P_G is the grid power without EV penetration. P_{EV} is positive when being charged, and negative when being discharged.

The constraints for the optimization are presented in (9)-(15).

(9) guarantees the EV battery is fully charged before the departure, while (10) makes sure that the battery SOC is between 0 and 1 during the whole process.

$$\int_{t_{HA}}^{t_{HD}} P_{EV\_Bat}(t) dt = (1 - S_R) E_{full} \tag{9}$$

$$0 \le S(t) = \frac{\int_{t_{HA}}^{t} P_{EV\_Bat}(x) dx}{E_{full}} \le 1 \tag{10}$$

where

$$P_{EV\_Bat} = \begin{cases} P_{EV\_Conv} \eta_{EV} & (Charging) \\ \dfrac{P_{EV\_Conv}}{\eta_{EV}} & (Discharging) \end{cases} \tag{11}$$

(12)-(13) are the power restrictions. (12) is for the unidirectional systems and (13) is for the bi-directional systems.

$$0 \le P_{EV\_Conv}(t) \le P_{\text{Ch\_max}} \tag{12}$$

$$-P_{Dis\_max} \le P_{EV\_Conv}(t) \le P_{\text{Ch\_max}} \tag{13}$$

where P_{Ch_max} is the maximum charging power and P_{Dis_max} is the maximum discharging power.

(14) is used for limiting the ramping rate of the grid load.

$$k_{dec\_lim} \le k_G(t) \le k_{inc\_lim} \tag{14}$$

where k_G is the grid power change rate, and k_{inc_lim}, and k_{inc_lim} are the grid power increasing and decreasing rate limits, respectively.

(15) guarantees that the total grid load is less than the maximum allowable load for the grid.

$$P_G(t) + P_{EV\_Conv}(t) \le P_{G\_lim} \tag{15}$$

where P_{G_lim} is the grid's maximum allowable load.

B. Algorithm Description

This algorithm is described based on the day-ahead load and EV profile. Taking unidirectional chargers as an example, the specific steps are listed in the following. Although the algorithm description is based on home charging unidirectional chargers, it can be applied for work charging and bi-directional chargers as well[13].

1. First, obtain an EV's parameters like t_{HD}, t_{WA}, t_{WD}, t_{HA}, S_R, etc. Then, as shown in Fig. 11(*a*), randomly scatter the charging power in the charging time zone, where the total charging energy should make the battery be fully chargerd before the departure. Then, rank the charging power in a descending order based on their corresponding TOU eletricity prices. For the same price, rank the one with a larger grid load first.

2. Shift one slice of #1 power (ΔP) to #N as shown in Fig. 11(*b*). As a result, the power in the zone with the highest price and largest grid load is shifted into the zone with the lowest price and lightest grid load. Note that ΔP is the minimum variation unit of the EV charging power, which can be detemined by the charger.

3. Then, check if constraints in (9)-(15), such as the power limits, and ramping rate, are satisfied. If so, confirm the action and then move to the next slice till all #1 power is shifted. If not, as shown in Fig. 11(*c*), withdraw the action and then orderly try to shift this slice to # N-1, #N-2, etc., till the constraints are met.

4. After the #1 power shift is done, as shown in Fig. 11(*d*), similarly shift #2 power, into #N, #N-1, etc. After #2 power shift is finished , then shift #3, #4, …, till #N-1. Then, the power shift of this EV is finished.

5. After this EV is finished, update the grid load by adding the EV charging power on it as shown in Fig. 11(*e*). Then, move to the next EV. Repeat the same actions described earlier. Till the load shifting of all the EVs are done, the charging profile for all EVs is created.

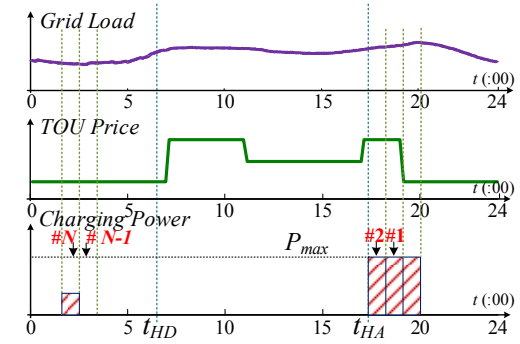

(*a*) *Step 1*

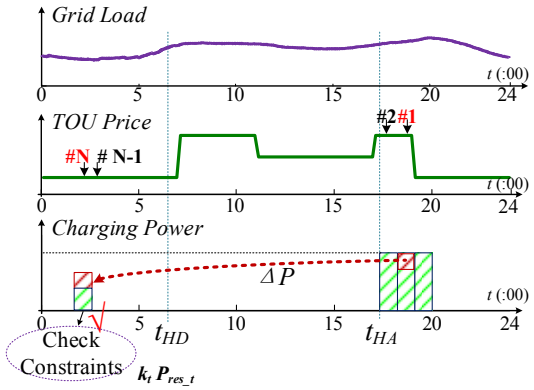

(*b*) *Step 2*

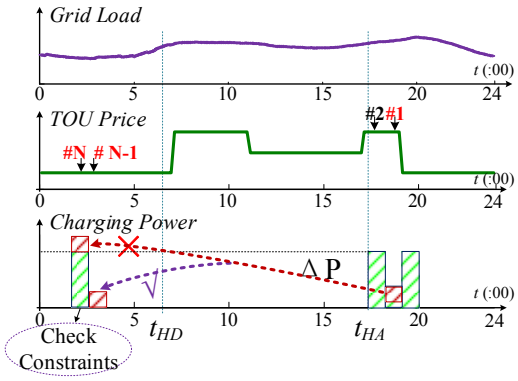

(*c*) *Step 3*

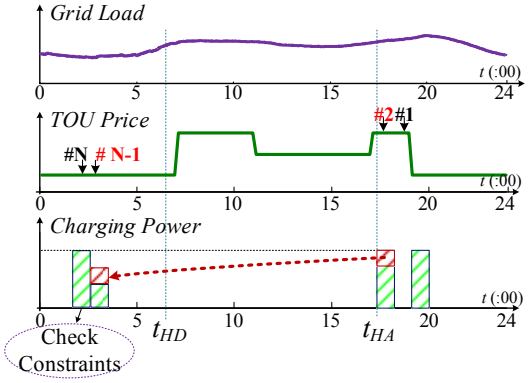

(*d*) *Step 4*

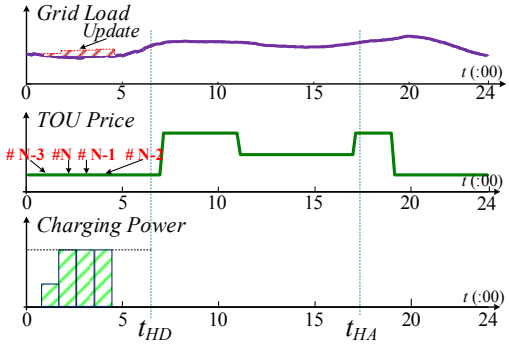

(*e*)

(*e*) *Step 5*

Fig. 11 Algorithm for the improved minimum-cost scheduling

Fig. 12 illustrates the system communication architecture. As can be seen, EVs transmit the information to the aggregator, like *trip patterns*, *SOCs*, *locations*, *battery capacities*, *charger levels*, etc. The aggregator receives the data from the utility side as well, such as the *day-ahead load demand*, *maximum load limits*, etc. Then, the aggregator uses these collected data to implement the optimization algorithm, which is proposed earlier. As a result, the charging and discharging schedules are created and the corresponding commands are sent to the EVs from the aggregator as shown in Fig. 12.

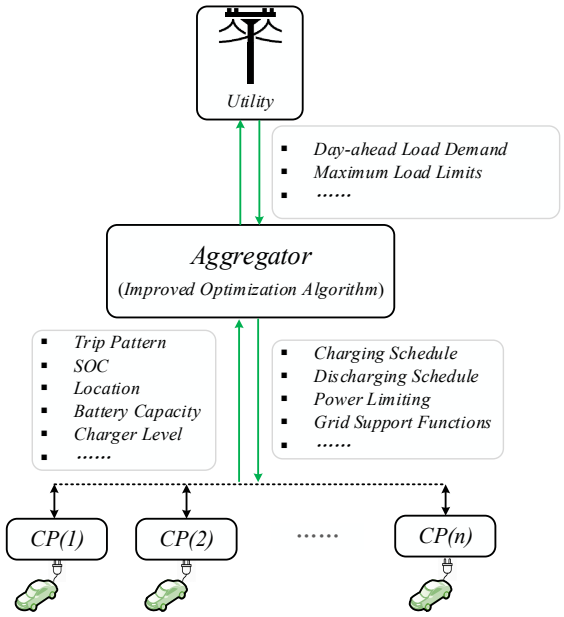

Fig. 12 System communication diagram (CP means charging point)

V. Simulation Results

The following presents the simulation results to verify the validity of the improved scheduling. The simulation parameters are the same as that shown in Table. I.

The results for the unidirectional charger in the cases of 30% and 100% EV penetrations are presented in Fig. 13(*a*)-(*b*). Compared with the conventional min-cost scheduling, the improved min-cost scheduling shifts the power surge to other low-price zone and correspondingly the maximum grid load is greatly reduced. In addition, the ramping rate is limited as well, which can help improve the grid's dynamic response and reduce the operating costs. Compared with 30% EV penetration, the grid load of 100% EV penetration is heavier, because of more EV charging power.

Furthermore, the grid's load ramping rate can be regulated by setting different ramping rate limits (see (19)). Fig. 13(*c*) presents the results of two ramping rates (30MW/min & 60MW/min). The maximum grid power for 30MW/min is slightly higher.

Fig. 13(*d*) presents the maximum grid load in cases of different EV penetrations. As can be seen, the maximum grid load is reduced from 3.20 to 1.20 for 100% EV penetration with the improved scheduling. Note that the maximum power is uniformed and the base is the maximum power when the penetration is 0%. It is also worth mentioning that the improved scheduling scatter the power surge into the same price zone, and thus the users' charging cost is maintained the same as that using convention scheduling, which is shown in Fig. 13(*e*).

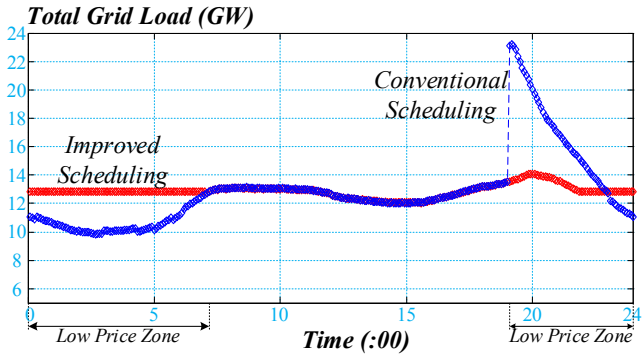

(*a*) *30% penetration*

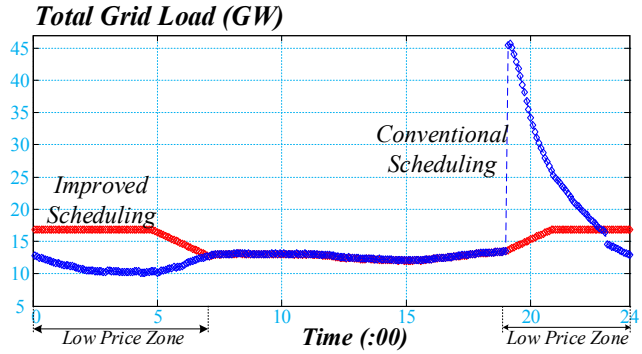

(*b*) *100% penetration*

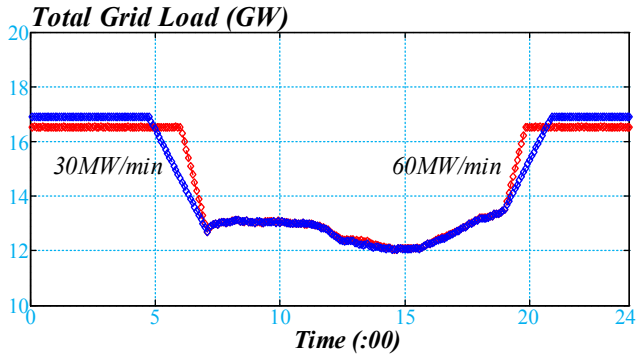

(c) Different ramp rates for 100% EV penetration

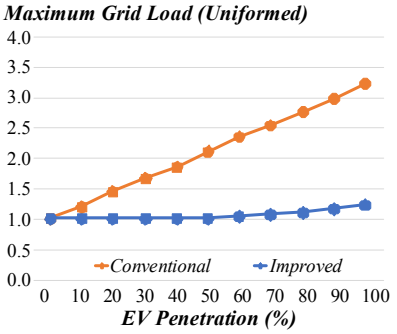

(d) Maximum grid load

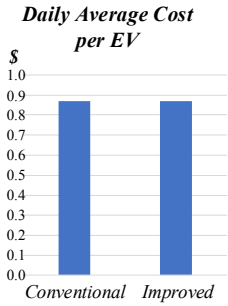

(e) Daily Average Cost

Fig. 13 Comparison of conventional and improved min-cost scheduling for unidirectional chargers

Similar results for the bi-directional systems are presented in Fig. 14. As can be seen in Fig. 14(*a*) for 30% EV penetration, the power surge is mitigated and the maximum grid power is

reduced greatly with the improved min-cost scenarios. Also, the ramping rate is restricted as well, which help improve the grid's dynamic response.

Fig. 14(*b*) presents the maximum grid load in the cases of different EV penetrations. It can be seen that the maximum is reduced from 3.5 to 1.3 with the improved min-cost scheduling, which alleviate the grid load greatly. Note that the maximum power is uniformed and the base is the maximum power when the penetration is 0%.

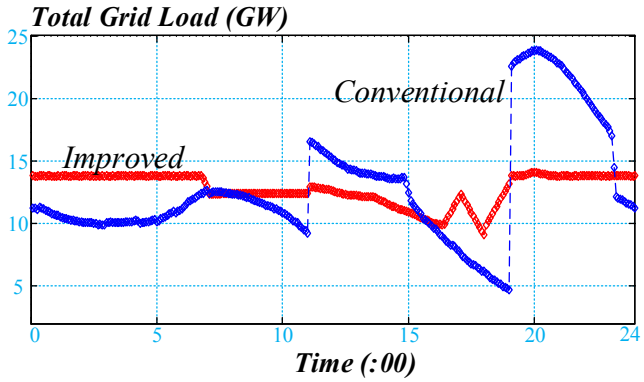

(a) 30% EV penetration

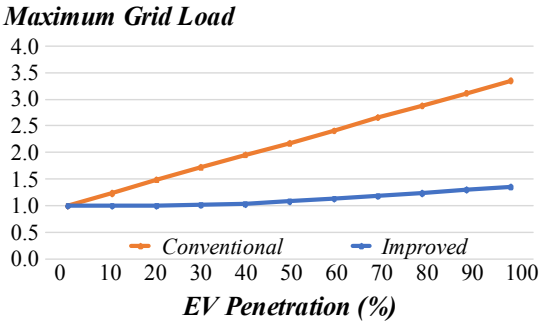

(b) Maximum grid load in cases of different EV penetrations

Fig. 14 Comparison of conventional and improved scheduling for bi-directional chargers

VI. Conclusion

In this paper, an EV mathematical charging cost model is first built with *TOU* electricity price, EV mobility and battery and charger specifications being taken into account. Then, with a conventional charging schedule of minimizing users' cost, the cost comparisons of uncoordinated chargers, scheduled unidirectional chargers, and scheduled bi-directional chargers are presented. It is observed that most users intend to charge the EVs as soon as the price is dropped into the low-price zone, and thus a great power surge occurs, which aggravates the load of the grid and worsens the grid's dynamic performance and operating costs. Therefore, an improved strategy is proposed to cope with these issues and the corresponding algorithm and communication architecture are illustrated. The simulations results show the power surge is reduced from 320% to 120% in the case of 100% EV penetration for unidirectional systems. In addition, the power ramping rate can be limited as well with the proposed scheme.

References

[1] E. Sortomme and M. A. El-Sharkawi, "Optimal charging strategies for unidirectional vehicle-to-grid," IEEE Trans. Smart Grid, vol. 2, no. 1, pp. 131–138, Mar. 2011.

[2] S. Han, S. Han, and K. Sezaki, "Development of an optimal vehicle-to-grid aggregator for frequency regulation," IEEE Trans. Smart Grid, vol. 1, no. 1, pp. 65–72, Jun. 2010

[3] E. Sortomme and M. A. El-Sharkawi, "Optimal scheduling of vehicle-to-grid energy and ancillary services," IEEE Trans. Smart Grid, vol. 3, no. 1, pp. 351–359, Mar. 2012.

[4] C. Wu, H. Mohsenian-Rad, and J. Huang, "Vehicle-to-aggregator interaction game," IEEE Trans. Smart Grid, vol. 3, no. 1, pp. 434–442, Mar. 2012.

[5] M. E. Khodayar, L. Wu, and M. Shahidehpour, "Hourly coordination of electric vehicle operation and volatile wind power generation in SCUC," IEEE Trans. Smart Grid, vol. 3, no. 3, pp. 1271–1279,Sep. 2012.

[6] Q. Li, T. Cui, R. Negi, F. Franchetti, andM. D. Ilic, "On-line decentralized charging of plug-in electric vehicles in power systems," in Proc. Optim. Control, 2011, pp. 1–12, CoRR

[7] Y. He, B. Venkatesh, and L. Guan, "Optimal scheduling for charging and discharging of electric vehicles," IEEE Trans. Smart Grid, vol. 3, no. 3, pp. 1095–1105, Sep. 2012.

[8] M. Erol-Kantarci and H. T. Mouftah, "Prediction-based charging of PHEVs from the smart grid with dynamic pricing," in Proc. IEEE 35th Conf. LCN, 2010, pp. 1032–1039.

[9] R. Jin, B. Wang, P. Zhang, and P. B. Luh, "Decentralized online charging scheduling for large populations of electric vehicles: A cyber-physical system approach," Int. J. Parallel, Emergent Distrib. Syst., vol. 28, no. 1, pp. 29–45, Feb. 2013.

[10] O. Sundstrom and C. Binding, "Flexible charging optimization for electric vehicles considering distribution grid constraints," IEEE Trans. Smart Grid, vol. 3, no. 1, pp. 26–37, Mar. 2012.

[11] K. Qian, C. Zhou, M. Allan and Y. Yuan, "Modeling of Load Demand Due to EV Battery Charging in Distribution Systems," in IEEE Transactions on Power Systems, vol. 26, no. 2, pp. 802-810, May 2011.

[12] A. Dubey and S. Santoso, "Electric Vehicle Charging on Residential Distribution Systems: Impacts and Mitigations," in IEEE Access, vol. 3, no., pp. 1871-1893, 2015.

[13] Y. Cao et al., "An Optimized EV Charging Model Considering TOU Price and SOC Curve," in IEEE Transactions on Smart Grid, vol. 3, no. 1, pp. 388-393, March 2012.